BULLETIN OF THE EARTHQUAKE
RESEARCH INSTITUTE
Vol. 55 (1980), pp. 681-703

29. *Geothermal Survey in and around O-ana Crater and Jodo-daira Flat, the Volcanoes Azuma.*

By Tsuneomi KAGIYAMA and Michinori HAGIWARA,

Earthquake Research Institute.

(Received September 10, 1980)

1. Introduction

The volcanoes Azuma, No. 8, 3-18 in the Catalogue of the World Active Volcanoes (KUNO, 1962), are a group of strato volcanoes and shield volcanoes and situated in the central part of the Northeastern Japan on the coordinate 37°44′N and 140°09′E (Fig. 1). In historic times, the eruptive activities were limitted to the Mount Issaikyo, though in documental records, neither explosions nor earthquake swarms associated with these volcanoes are very frequent. Scientific investigations were made at the time of the activities of 1893, 1950, and 1966 (YOKOYAMA, 1893a, 1893b; MINAKAMI and HIRAGA, 1951; OHNO, 1971), and Fukushima Prefecture Disaster Prevention Committee (1979) reviewed these events. Our mension should also be made of two scientists, who were killed by steam explosion in 1893. On December 7, 1977, a minor steam explosion took place at O-ana crater, southestern part of the Issaikyo, after 11 years of dormancy. The increase of fumarolic cloud since February, 1977 was reported by the Fukushima Local Meteorological Observatory (1978).

This kind of precursory geothermal activities was often reported, in conjunction with the former eruptions of Azuma and with various other volcanoes. These evidences suggest a close relation between volcanic eruption and geothermal activity. The importance of frequent monitoring of geothermal activity for the prediction of volcanic eruptions has been emphasized. For this purpose, a geothermal survey was conducted in October, 1979, to make disclose the surface and near-surface temperature distributions and heat discharge rate around O-ana crater and Jodo-daira.

2. Survey Methods and Analysis

As summarized in Table 1, the present survey consisted of the surface temperature distribution by an IR radiometer, the 1-meter depth tempera-

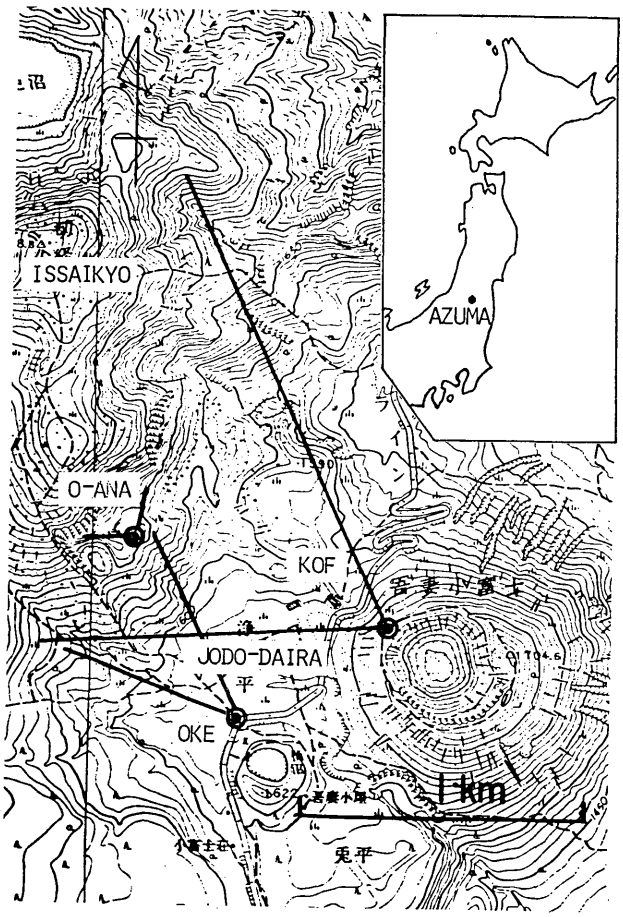

Fig. 1. Topographic map around Mt. Issaikyo showing the volcanoes Azuma and the observation sites. Surface temperature was measured from the three points, Kof, O-ana and Oke.

Table 1. Outlines of the geothermal survey of the volcanoes Azuma in October 1979.

Subject	Conducted works	Date	Means of measurement
Distribution of thermal anomaly	Sight obs.	Oct. 16	
	Ground temperature	Oct. 17-24	Thermistor probe
	Surface temperature		IR radiometer
Heat discharge rate	O-ana pt.	Oct. 20	ERI type Ground Scanner
	Kof pt.	Oct. 22	
	Oke pt.	Oct. 23	
	Rising speed of fume clouds	Oct. 23	Successive photographing

Table 2. Specifications of ERI type Infra-red Ground Scanner.

Detector	thermistor bolometer
optical band	8—12.5 μm
response speed	10 ms
Range of temperature	−20 to 1500°C (4 steps)
Reliability	±0.5°C
Field of view	5 mrad
Horizontal scanning	motor-driven or manual
range of scanning	360° in angle
angular velocity	high 1.10 mrad/s
	low 0.72 mrad/s
Vertical scanning	manual
Accuracy scanning	0.1 degree in angle
Noise level	0.05 mV
Recorder	ink writing recorder
	magnetic tape data recorder
Total power consumption	30 W
Total weight	30 kg

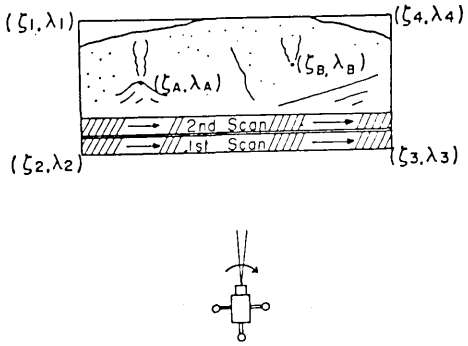

Fig. 2. Schematic illustration of the scanning and the angle coordinates.

ture distribution by thermistor probes, and the rising speed of fume clouds by successive photographs. These data were analyzed to estimate the heat discharge rate of the area.

2-1. Surface temperature distribution

ERI-type IR ground scanner, on which a commercial-type infrared radiometer substitutes for the telescope of the ballon theodolite was used for the present survey (Table 2).

Measurement

The coordinates ($\zeta_{1\cdots4}$, $\lambda_{1\cdots4}$) of every corner of the measured area were determined on the theodolite scales by referencing polaroid pictures.

Throughout this data analysis, the angle readings on the theodolite dials are referenced. The coordinates of active vents and other remarkable features ($\zeta_{A,B,\cdots}$, $\lambda_{A,B,\cdots}$) were also determined. Then, the first motordriven horizontal scan was made, with the vertical angle fixed as shown by Fig. 2. The temperature between λ_2 and λ_3 was registered on the recorder. After changing the vertical angle (1 degree intervals is usual), the second run was made. By repeating this procedure, the spatial temperature distribution $T(\zeta, \lambda)$ is obtained. Additional measurements were also manually carried out on each point of interest. Then, by interpolating the measured data with linear function, the temperature at grid points at every 0.1 degree intervals, which is the maximum resolution of the theodolite, were presented. A contour map of temperature distribution

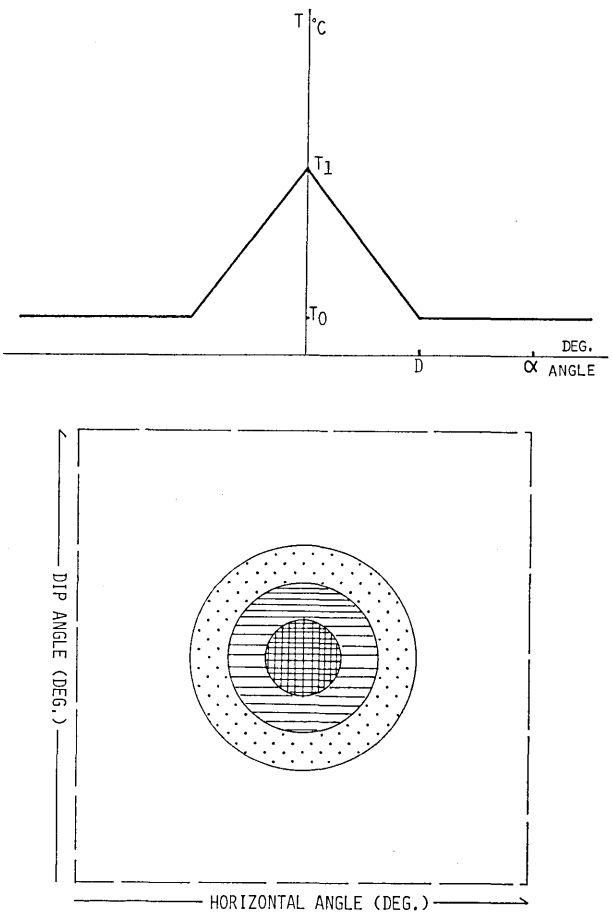

Fig. 3a. A simple model of the surface temperature distribution. Surface temperature is measured within the area surrounded by the broken line.

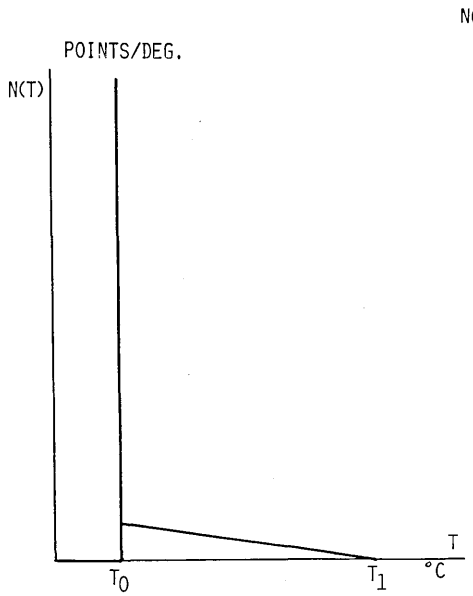

Fig. 3b. Frequency distribution of the grid temperature for the Fig. 3a model. The observation error is none.

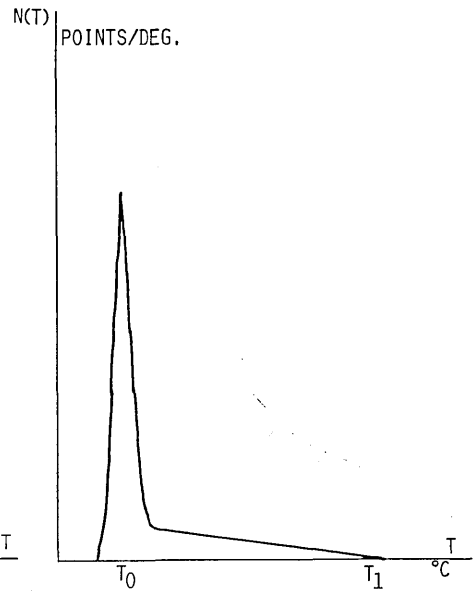

Fig. 3c. Frequency distribution of the grid temperature. The observation error is of normal distribution with the deviation σ_T.

was drawn from these grid point temperature data.

Determination of the normal temperature T_0 and standard deviation σ_T

For the quantitative analysis of the surface temperature distribution, the temperature at thermally normal point and the error of obtained temperature should be determined (KAGIYAMA et al., 1979). If the surface temperature distribution is given as in Fig. 3a, the expected frequency distribution of the measured temperature, $N(T)$, is presented in Fig. 3b or by 3c. Fig. 3b represents a case where no error is included, and Fig. 3c represents the case where the obtained temperature accompany a certain fluctuation formulated by

$$f(T)dT=\frac{1}{\sqrt{2\pi}\,\sigma_T}\exp\left[-\frac{(T-T_r)^2}{2{\sigma_T}^2}\right]dT\,, \tag{1}$$

where f is the possibility that the temperature is measured between T and $T+dT$ when the true temperature is T_r. σ_T is the deviation of the measurement error due to, for example, equipment noise, difference of emissivity of the ground surface, and the effect of the difference of the micrometeorological conditions of the near surface. When the measure-

ment is made over a sufficiently wide area compared with the thermally anomalous area (1.5 times in usual), the peak position in Fig. 3c becomes sufficiently close to T_0, and the distribution pattern $N(T)$ can be formulated by

$$\log N(T) = -\frac{(T-T_0)^2}{2\sigma_T^2} + \text{const.} \tag{2}$$

T_0 and σ_T are detemined by least square fitting of the formula (2) to the given observation data. In actual cases, those data that are not between $T_0-3\sigma_T$ and $T_0+\sigma_T$ are eliminated, and the above procedure is repeated until satisfactory results are finally obtained.

2-2. Estimation of heat discharge rate

Two evaluation methods for fumarolic zones and steaming grounds are used for the present study.

a. Fumarolic zones

Fumarolic clouds can be regarded to rise as a continuous plume. The relation between the thermal energy release rate Q [watt] and the plume rise height h [m] was given by BRIGGS (1969) as,

$$Q = 2.7\times10^4 \frac{h^3u^3}{x^2}, \tag{3}$$

where x [m] is the horizontal distance from the heat source and u [m/sec] is the wind velocity. These parameters can be obtained by analyzing the plume shape on a photograph. However, each value of x, u, and h includes considerable uncertainty, the authors modified this formula as,

$$h = C_1 \cdot x^{2/3}, \quad Q = 2.7\times10^4 \cdot C_1^3 \cdot u^3, \tag{4},$$

$$h = C_2 \cdot t^{2/3}, \quad Q = 2.7\times10^4 \cdot C_2^3 \cdot u, \tag{5},$$

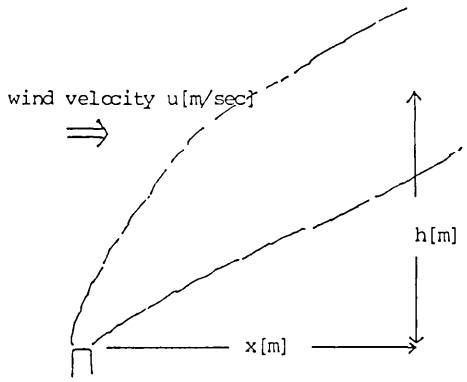

Fig. 4. Schematic illustration of a plume rise.

where t [sec] is the time after the marked position of the plume is effused from the vent. C_1 and C_2 are the coefficients which were determined from the rise pattern of fumarolic plume. For simplifying the photo reduction procedure, this formula is further modified as,

$$h'=C_1'\cdot x'^{2/3},\ Q=2.7\times10^4\cdot C_1'^3\cdot m\cdot u^3, \tag{6}$$

$$h'=h_0'+h_1'=C_2'\cdot t^{2/3},\ Q=2.7\times10^4\cdot C_2'^3\cdot m^3\cdot u, \tag{7}$$

where m is a reduced scale, $m=h/h'=x/x'$, and h' and x' are the height and horizontal distance in the scale m. In the formula (7), h' is divided into two parts as the height of favorable level for analysis from the vent, h_0', and the rise height, h_1', of plume from the level, h_0'.

Method 1

Estimation method using the formula (6) is presented as follows.

1) A photograph of a desired plume is taken.

2) The reduction scale m is determined from a well-known distance on the picture.

3) The coefficient C_1' is determined by the best fitting of the curves, $h'=C_1'x'^{2/3}$, to the plume shape.

4) The wind velocity is determined by tracking the plume shape on successive photographs or by the meteorological observation.

5) Heat discharge rate, Q, is obtained by formula (6).

Method 2

Estimation method using the formula (7) is as follows.

1) Photographs of a desired plume are taken successively, at the same time intervals (5 or 10 seconds in usual).

2) The h_1' of several remarkable points of the plume are read on the successive photographs and $h_1'-t$ curves are plotted.

3) The coefficient C_2' is determined by the best fitting of the curves, $h'=C_2't^{2/3}$.

4) The m and u are determined.

5) The average value of Q is obtained by the formula (7).

b. Steaming ground

Heat discharge rate from steaming grounds can be calculated according to the formula by SEKIOKA and YUHARA (1974),

$$Q=K\Sigma\Delta\theta\cdot S, \tag{8}$$

where $\Delta\theta$ is the temperature difference from the thermally normal point,

$S[m^2]$ is the area with $\Delta\theta$, and K is a coefficient depending on the meteorological conditions. SEKIOKA et al (1978) suggested that the coefficient K ranged from 2×10^{-4}[cal·sec^{-1}·cm^{-2}·deg^{-1}] to 2×10^{-3}[cal·sec^{-1}·cm^{-2}·deg^{-1}] and the average value was determined as 8×10^{-4}[cal·sec^{-1}·cm^{-2}·deg^{-1}] from the former observations. In the present paper, the surface temperature of the thermally normal point corresponds to T_0 in the last section, 2-1, and thermal anomaly is defined as the area whose temperature is higher than $T_0+3\sigma_T$. Q can be estimated by the following formula:

$$Q=34\cdot\sum_{Ti>T_0+3\sigma_T}(T_i-T_0)\cdot N(T_i)\cdot A\,, \qquad (9)\,,$$

Fig. 5a. View of the southeast flank of Mt. Issaikyo and Jodo-daira flat. Surface temperature was measured over the area surrounded by the broken line.

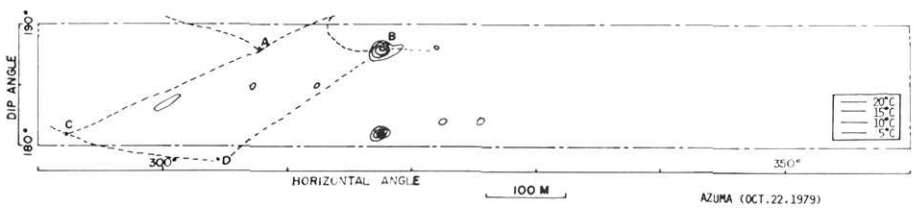

Fig. 5b. Surface temperature distribution observed from Kof point. The contour interval is every 5°C. The lowest contour line represents 5°C.

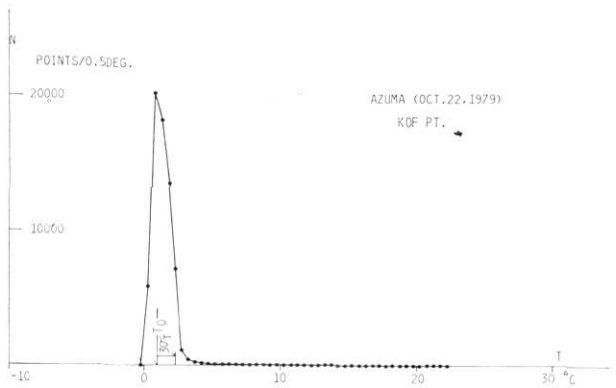

Fig. 5c. Frequency distribution of grid temperature measured from Kof point. One grid point represents the area which corresponds to 0.1° by 0.1° of vertical and horizontal angles from Kof point.

(continued from back cover)

BULLETIN OF

THE EARTHQUAKE RESEARCH INSTITUTE

UNIVERSITY OF TOKYO

Vol. 53, Part 3. 1978.

Contents.

The Izu-Oshima-kinkai Earthquake of 1978.

Papers and Reports.

(continued inside back cover)

(For the papers written in Japanese or in occidental languages, the abstracts are given in occidental languages or in Japanese respectively.)

a. Kof pt.

Fig. 5a is the view from Kof point at daytime. There are many altered zones and pits, remnants of the previous minor explosions around the southeast flank of the Issaikyo. The temperature was measured widely to cover the whole area around Jodo-daira and O-ana crater within the broken line in Fig. 5a. Fig. 5b shows the surface temperature distribution obtained from Kof point. The angle coordinates of the marked points in Fig. 5b are presented in Table 3a. The frequency of temperature $N(T)$ is presented in Fig. 5c and Table 3b. Through the analysis of $N(T)$, normal temperature T_0 and standard deviation σ_T were deter-

Table 4a. Meteorological conditions during the observation from O-ana pt.

Time	Air temp. (°C)	Wet bulb temp. (°C)	Humidity (mm Hg)
Oct. 20 17 : 37	5.5	4.0	5.4
17 : 55	5.2	4.0	5.5
18 : 13	5.2	4.0	5.5
18 : 30	5.0	4.2	5.8
18 : 48	5.0	4.3	5.9
19 : 08	5.0	4.7	6.2
19 : 27	4.8	4.3	6.0
19 : 46	4.6	4.2	6.0
20 : 00	4.7	4.2	5.9
20 : 12	4.7	4.2	5.9
20 : 25	4.8	4.2	5.9
20 : 31	4.8	4.2	5.9
20 : 38	5.0	4.0	5.6
20 : 48	5.2	3.8	5.3
21 : 03	5.6	3.4	4.8
21 : 18	6.6	3.0	3.9
21 : 32	6.4	2.8	3.8
21 : 38	5.8	3.2	4.5
21 : 42	5.5	3.2	4.6

Table 4b. View positions of marked points in view angle coordinates from O-ana point.

Point	Dip angle* (in degree)	Horizontal angle* (in degree)	Remarks
A	183.4	200.8	Active fumarole
B	183.2	224.1	
C	175.8	257.6	
D	173.0	283.7	

* Angles are measured from an arbitrary direction.

Table 4c. Frequency distribution of the temperature measured from O-ana point.

Temp. °C	N(T) points		Temp. °C	N(T) points		Temp. °C	N(T) points	
−4.5	0	0*	15.5	5066	3908*	35.5	49	5*
−3.5	0	0	16.5	3638	2617	36.5	36	7
−2.5	0	0	17.5	2723	1772	37.5	24	3
−1.5	0	0	18.5	2307	1532	38.5	21	3
−0.5	0	0	19.5	1595	1033	39.5	13	0
0.5	35	35	20.5	1227	793	40.5	9	0
1.5	29	29	21.5	842	468	41.5	4	0
2.5	31	31	22.5	659	284	42.5	3	0
3.5	24	24	23.5	509	199	43.5	0	0
4.5	26	26	24.5	405	137	44.5	1	0
5.5	27	27	25.5	321	103	45.5	0	0
6.5	29	29	26.5	283	84	46.5	0	0
7.5	2871	2311	27.5	211	59			
8.5	30322	20740	28.5	183	63			
9.5	41629	21314	29.5	160	53			
10.5	43962	26294	30.5	120	36			
11.5	41085	32521	31.5	89	23			
12.5	25432	21721	32.5	80	17			
13.5	11198	8998	33.5	68	13			
14.5	7031	5375	34.5	64	13			

* Selected area (Horizontal angle >220°)
One point represents 0.072 m².

mined as 1.0°C and 0.4°C, respectively. Geothermal anomaly is determined as the area where the temperature is higher than $T_0+3\sigma_T$, 2.2°C. Such anomalies detected in Fig. 5b are only at O-ana crater (point B), Tsubakuro-sawa (between point A and point C), and at the area indicated by horizontal angle, 318° and vertical angle, 180°. Meteorological conditions during the observation could not be measured because of the strong typhoon wind.

b. O-ana pt.

Fig. 6a shows the view from O-ana point. Surface temperature was measured over the area within the broken line. Fig. 6b shows the obtained surface temperature distribution. The ambient temperature and the humidity during the observation and the positions of the marked points are presented in Tables 4a and 4b, respectively. By the analysis of the frequency of temperature $N(T)$ presented in Fig. 6c and Table 4c, T_0 and σ_T were determined as 10.2°C and 1.2°C, respectively. Thermal

anomaly where temperature is higher than 13.8°C roughly corresponds to the area surrounded by 15°C contour line in Fig. 6b. Such anomalies are detected at point A, which is the most active fumarole, and at the area on the right side of the point B, which is a minor fumarole group

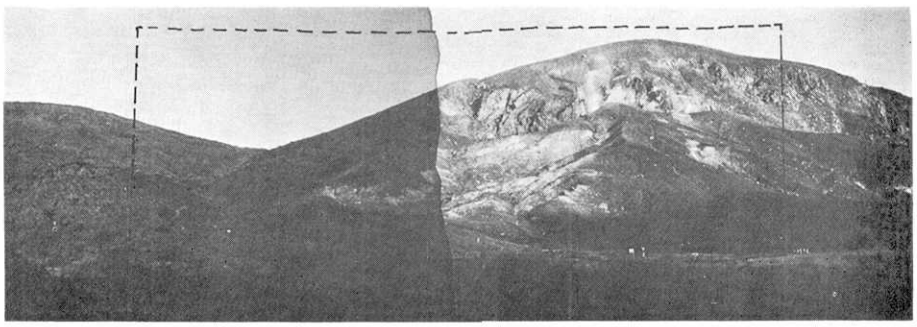

Fig. 7a. Tsubakuro-sawa geothermal area viewed from Oke point. Surface temperature was measured over the area surrounded by the broken line.

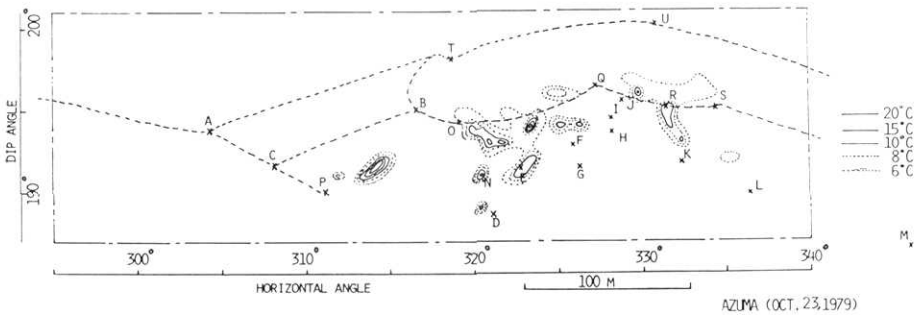

Fig. 7b. Surface temperature distribution of Tsubakuro-sawa obtained from Oke point. Contour intervals of the solid line and the broken line are every 5°C and 2°C, respectively. The lowest solid and broken contour lines represent 10°C and 6°C, respectively.

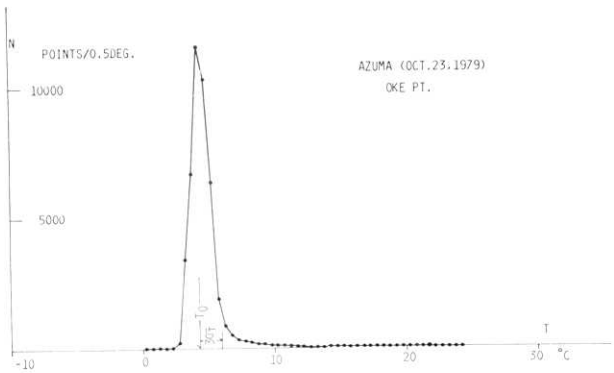

Fig. 7c. Frequency distribution of grid temperature measured from Oke point. One grid point represents 2.5 m^2.

Table 5a. Meteorological data during the observation from Oke pt.

Time	Air temp. (°C)	Wet bulb temp. (°C)	Humidity (mm Hg)
Oct. 23 04 : 30	−0.6	−1.2	3.9
04 : 36	0.0	−1.0	3.8
04 : 42	−2.0		
04 : 50	−2.0		
05 : 03	−2.5	−2.6	3.8
05 : 10	−2.6	−3.0	3.5
05 : 26	−2.5	−2.6	3.8
05 : 35	−1.0	−1.5	3.9
06 : 04	−1.4		
06 : 06	−1.8		
06 : 12	−3.0		

Table 5b. View positions of marked points in view angle coordinates from Oke point.

Point	Dip angle* (in degree)	Horizontal angle* (in degree)	Remarks
A	194.0	304.5	
B	195.1	316.7	
C	191.8	308.3	
D	188.6	321.2	
E	191.5	322.9	
F	192.8	326.0	Ground temp. meas. pt. #21
G	191.5	326.4	#22
H	193.7	328.3	#17
I	194.5	328.3	#19
J	195.5	328.9	#20
K	191.8	332.5	#18
L	189.9	336.5	#16
M	186.5	346.0	#14
N	190.6	320.4	#27
O	194.2	319.2	
P	190.0	311.3	
Q	196.4	327.4	
R	195.0	331.8	
S	195.1	334.5	
T	198.1	318.8	
U	200.1	330.9	

* Normal directions are derived from D−184.9° and H−1.0°, respectively.

Table 5c. Frequency distribution of the temperature measured from Oke point.

Temp. °C	N(T) points	Temp. °C	N(T) points	Temp. °C	N(T) points
−4.75	0	5.25	6346	15.25	14
−4.25	0	5.75	1952	15.75	13
−3.75	0	6.25	872	16.25	4
−3.25	0	6.75	541	16.75	10
−2.75	0	7.25	335	17.25	4
−2.25	0	7.75	285	17.75	4
−1.75	0	8.25	229	18.25	6
−1.25	0	8.75	190	18.75	2
−0.75	0	9.25	170	19.25	3
−0.25	0	9.75	124	19.75	3
0.25	30	10.25	103	20.25	1
0.75	7	10.75	100	20.75	1
1.25	9	11.25	80	21.25	1
1.75	7	11.75	58	21.75	2
2.25	31	12.25	55	22.25	0
2.75	230	12.75	39	22.75	0
3.25	3432	13.25	37	23.25	0
3.75	6710	13.75	18	23.75	1
4.25	11576	14.25	25	24.25	0
4.75	10330	14.75	11	24.75	0

One point represents 2.5 m^2.

and steaming ground. The maximum temperature recorded at point A was 45°C.

c. Oke pt.

At Tsubakuro-sawa, geothermal activity has continued since the eruption of 1893. Surface temperature was measured over Tsubakuro-sawa within the broken line in Fig. 7a from Oke point. The ambient temperature and the humidity are presented in Table 5a. Fig. 7b shows the obtained temperature distribution. The positions of the marked points are presented in Table 5b. Through the analysis of $N(T)$ presented in Fig. 7c and Table 5c, T_0 and σ_T were determined as 4.3°C and 0.6°C, respectively, then the area higher than 6.1°C is defined as thermal anomaly. Such anomalies were detected near point P and within the triangle area of points O, Q, and D. Another anomaly between the points R and K corresponds to the geothermal activity of the outer wall of O-ana crater, which is near the O-ana point, and was not covered in

the previous result of O-ana point. No other anomaly was detected from Oke point. At the largest crater of the 1893 eruption, northwest of Tsubakuro-sawa, which was not measured in the present study, no geothermal activity was recognized during sight observation.

3-2. 1 m depth ground temperature distribution

Although the ground temperature measurements need more time than the surface temperature measurements, the ground temperature is more stable to allow us to detect lower level of geothermal anomaly (order of 10 HFU). The 1 m depth ground temperature was measured at 37 points by the present survey as shown in Table 6. The positions of the observation points were determined by portable transit. Fig. 8 shows the result. We could not survey the whole area over O-ana crater and Jodo-daira because of limited observation time. Thermal anomalies detected by IR observations and sight obseration are also presented by the dotted area in Fig. 8. It is roughly considered that the heat discharge rate from these anomalies is larger than several hundreds HFU and these areas correspond to the area where ground temperature is higher than 25°C. It is clear that a zone of thermal anomaly extends from Tsubakuro-sawa

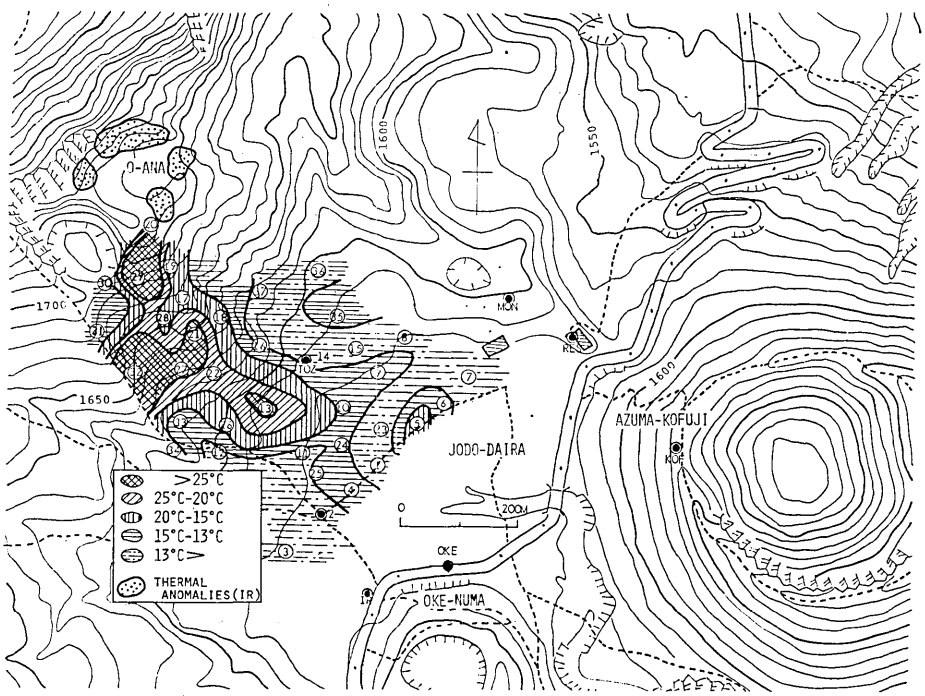

Fig. 8. 1 m depth ground temperature distribution around Jodo-daira.

Table 6. 1 m depth ground temperature.

Site No.	Local coordinates X(m)	Y(m)	Set. time	Meas. time	Temp. °C	Thermistor ID No.	Hole depth
1	98	87	17 12 : 54	20 09 : 56	11.7	76E-10	
2	0	0	17 13 : 11	20 11 : 27	12.6	E-17	
3	−65	−67	17 13 : 20	20 11 : 21	11.4	E-08	
4	47	42	17 13 : 32	20 11 : 32	14.2	E-05	
5	161	161	17 13 : 42	20 11 : 38	17.6	E-04	
6	201	197	17 13 : 53	20 11 : 44	13.3	E-18	
7	242	232	17 14 : 30	20 11 : 48	11.1	E-15	
				22 17 : 18	11.0		
				24 05 : 40	10.8		
8	135	309	17 14 : 53	20 11 : 54	12.4	E-02	
9	86	249	17 15 : 23	20 12 : 02	14.0	E-01	
10	30	189	17 15 : 33	20 12 : 15	14.7	E-06	1.0 m
					12.1	E-23	0.5 m
11	−41	109	17 16 : 12	20 14 : 34	12.6	E-24	
12	−182	102	17 16 : 38	20 14 : 22	12.3	E-13	
13	−108	182	17 16 : 56	20 12 : 27	26.0	E-22	1.0 m
					20.9	E-21	0.5 m
14	−30	267	17 17 : 06	20 14 : 50	11.5	E-12	
				22 10 : 10	11.4		
				24 05 : 32	11.3		
15	53	287	18 09 : 59	20	12.0	E-11	1.0 m
					11.5	E-09	0.5 m
16	−115	292	18 10 : 23	20 14 : 58	12.0	E-07	
17	−251	370	18 10 : 46	20	15.4	E-16	
18	−185	342	21 11 : 25	22 10 : 26	15.6	E-02	
19	−274	425	21 12 : 05	22 10 : 41	18.2	E-08	
20	−306	493	21 12 : 36	22 10 : 58	20.1	E-18	1.0 m
					17.7	E-17	0.7 m
21	−226	309	21 12 : 59	22	28.6	E-19	1.0 m
					17.8	E-14	0.4 m
22	−195	237	21 13 : 14	22 11 : 44	23.0	E-16	1.0 m
					16.8	E-05	0.5 m
23	98	152	22 14 : 00	23 14 : 00	11.7	E-09	
24	27	122	22 14 : 03	23 14 : 05	13.2	E-04	
25	−5	68	22 14 : 09	23 14 : 08	13.6	E-02	
26	−168	153	22 14 : 20	23 14 : 14	15.9	E-23	
27	−254	249	22 14 : 29	23 14 : 20	28.2	E-16	
28	−286	340	22 14 : 44	23 14 : 26	16.7	E-08	1.0 m
					11.8	E-17	0.5 m
29	−325	406	22 14 : 53	23 14 : 40	62.4	E-18	
30	−390	400	22 15 : 11	23 14 : 45	11.8	E-11	

(Continued)

Site No.	Local coordinates X(m)	Y(m)	Set. time	Meas. time	Temp. °C	Thermistor ID No.	Hole depth
31	−398	315	22 15 : 50	23 14 : 43	11.7	E-24	
32	−325	241	22 16	23 14 : 55	43.0	E-10	
33	−248	155	22 16 : 20	23 15 : 00	13.7	E-13	
34	−259	108	22 16 : 35	23 15 : 03	15.5	E-22	
35	12	344	23 16 : 10	24 05 : 18	13.6	E-02	1.0 m
					10.4	E-04	0.5 m
36	−11	425	23 16 : 24	24 05 : 25	12.7	E-10	1.0 m
					9.5	E-13	0.5 m
37	−116	386	23 16 : 38	24 05 : 07	12.5	E-22	1.0 m
					10.3	E-08	0.5 m

X: Distance from the point ♯2, positive to the east.
Y: Distance from the point ♯2, positive to the north.
Set. time: The time when the thermistor probe was inserted.
Meas. time: The time when the temperature was measured.

to O-ana crater and that Jodo-daira is the cold area, except the area of a branch extension of Tsubakuro-sawa anomaly due to the influence of hot water stream.

3-3. Thermal energy release rate

For monitoring the thermal activity, not only the distribution but also its 'intensity' should be measured. Therefore, the thermal energy release rate from around O-ana crater was estimated.

a. O-ana crater

As shown by Fig. 6b, the area of the thermal activities of O-ana crater is divided into two part, the fumarole at point A and steaming ground at the right side of point B. Formulae (6) and (7) were included in the former region and formula (9) was in the latter region.

The fumarole at point A emits the plume whose shape is shown in Fig. 9a. Fig. 9b shows the trajectories of remarkable points of the fumarolic plume in the successive photographs. The rise patterns of these points are quite stable. The rise height on photographs, h_1', at each point is plotted is Fig. 9c. By fitting the $h'-t$ curves to the rise pattern of each point, C_2' is determined. Reduction scale m and wind velocity u are determined as 810 and 1.2 [m/sec]. Q is estimated to be 5.7×10^6 watt as the average of values for each point by the formula (7) as shown in Table 7. Another method, applying formula (6), presents the following result. By fitting the $h'-x'$ curves to the plume shape on the projected photoslide (in this case, $m=405$), C_1' is determined to be

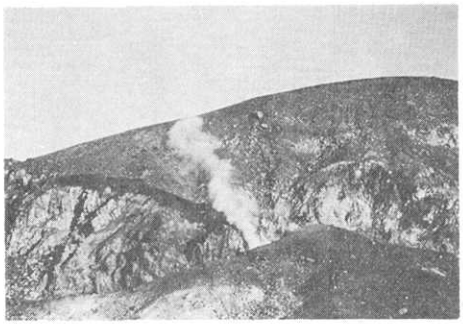

Fig. 9a. A fumarolic plume of O-ana, October 23, 1979.

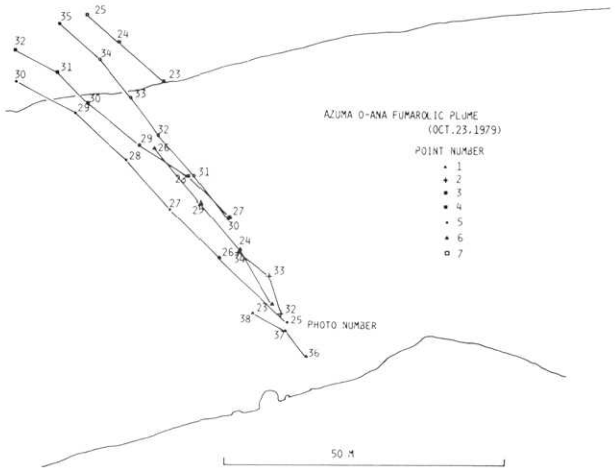

Fig. 9b. Trajectories of seven marking points of a fumarolic piume.

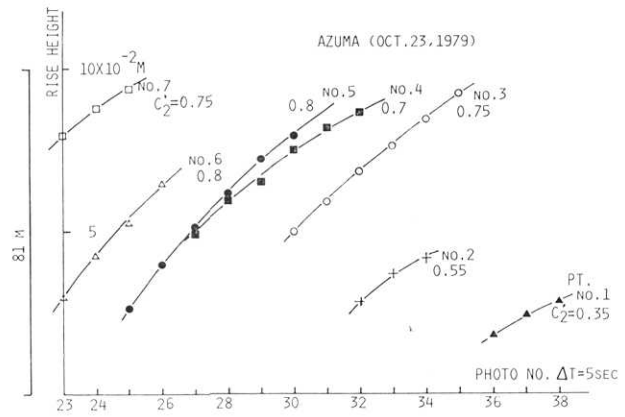

Fig. 9c. Rise height of the marking points of the fumarolic plume in Fig. 9b. Coefficient C_2' can be determined by the best-flt with varing C_2'.

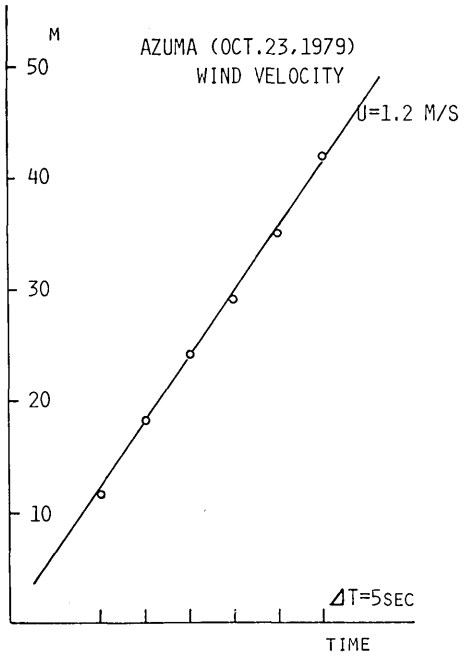

Fig. 9d. Determination of the wind velocity on October 23, 1979.

0.7. Heat discharge rate is obtained as 5.9×10^6 watt. As the average of two estimates, Q is estimated at 5.8×10^6 watt.

For another region at right side of point B, Q is determined as 3.0×10^5 watt by the formula (9), where the area size corresponds to one grid point, A, is assumed to be 0.072 [m^2/point].

b. Tsubakuro-sawa

Q is determined as 1.1×10^6 watt by the formula (9) for the area size of one grid point is assumed to be 2.5 [m^2/point]. Table 8 summarizes present estimation.

4. Summary

The results of the present survey are summarized as follows.

1) Surface temperature distribution and ground temperature distribution at 1 m depth were obtained. The existence of a zone of thermal anomalies in the area from O-ana crater to Tsubakuro-sawa was clarified.

2) Thermal energy release rate from O-ana crater and from Tsubakuro-sawa were estimated to be 6.1×10^6 watt and 1.1×10^6 watt, respectively. Heat discharge rate of Mount Issaikyo was evaluated at 7.2×10^6

Table 7. Data of the determination of fumarolic heat discharge rate from O-ana.

Photo No.	Rise height (cm)							
	1	2	3	4	5	6	7	
21								
22								
23						2.95	7.90	
24						4.20	8.75	
25					2.60	5.20	9.35	
26					4.00	6.40		
27				4.95	5.55			
28				5.90	6.10			
29				6.50	7.20			
30			4.95	7.45	7.90			
31			5.90	8.15				
32		2.85	6.80	8.60				
33		3.65	7.55					
34		4.15	8.40					
35			9.15					
36	1.80							
37	2.40							
38	2.80							
C_2'	0.35	0.55	0.75	0.70	0.80	0.80	0.75	(10^{-2})
C_2	0.70	2.7	6.9	5.6	8.4	8.4	6.9	(MW)

Average Q_2=5.7 MW m=810, U=1.2 m/s
Photographs were taken at every 5 seconds.

Table 8. Heat discharge rate from the Mt. Issaikyo area.

Site name	Heat discharge rate (MW)	Site discription
O-ana	5.8	Fumarole
	0.3	Steaming ground
Tsubakuro-sawa	1.1	Steaming ground
Total	7.2	

watt in October, 1979. This amount is one order small in magnitude compared with the volcanoes Kuju or Kirishima, which have remarkable geothermal activities.

3) After VOLCANOL. CENTER (1979), the volcanoes Azuma remained active after the eruption of December 1977, however, since 1979, its activity has decreased. It is considered that the present result represents the thermal state of the volcano Azuma-issaikyo at the lower level of its activity.

5. Acknowledgements

The authors are grateful to Prof. Takagi, Dr. Mishina and Dr. Uyeki, Univ. of Tohoku, for their kind considerations of our observations. We also thank Prof. Shimozuru, Prof. Hagiwara, Dr. Watanabe and Mr. Miyazaki of our institute for critically reviewing our manuscript. Dr. Watanabe also helped us with observations.

References

BRIGGS, G.A., 1969. Plume rise, *Critical Review Series, Rep.* TID-25075. At. Energy Comm. Washingnton, D.C.

FUKUSHIMA LOCAL METEOROLOGICAL OBSERVATORY, 1978. Volcanic activity of Azumayama in 1977 (in Japanese). *Rep. Coordinating Comm. Prediction of Volcanic Eruptions*, **12**, 45-47.

FUKUSHIMA PREF. DISASTER PREVENTION COMM., 1979. Rep. Volcanic activity of Azumayama (in Japanese).

KAGIYAMA, T., K. UHIRA, T. WATATABE, F. MASUTANI and M. YAMAGUCHI, 1979. Geothermal survey of the volcanoes Kirishima (in Japanese). *Bull. Earthq. Res. Inst.*, **54**, 187-210.

KUNO, H., 1962. Catalogue of the active volcanoes of the world including solfatara fields, Part XI Japan, Taiwan and Marianas. Inter. Assoc. Volcanol. Rome.

MINAKAMI, T. and S. HIRAGA, 1951. The minor activity of Volcano Azuma in February 1950. *Bull. Earthq. Res. Inst.*, **29**, 383-391.

OHNO, Y., 1971. Temporary observation of Volcano Azumayama (1966) (in Japanese). *Tech. Rep. of Japan Meteorol. Agency*, **75**, 62-72.

SEKIOKA, M. and K. YUHARA, 1974. Heat flux estimation in geothermal area based on the heat balance of the ground surface. *J. Geophy. Res.*, **79**, 2053-2058.

SEKIOKA, M., Y. ITO, T. SAITO, M. OBA and K. TAKAHASHI, 1978. Measurement of heat discharge at Owakudani geothermal area, Hokone Volcano, Japan (in Japanese). *J. Japan Geotherm. Energy Assoc.*, **15**, 11-18.

SHIMOZURU, D. and T. KAGIYAMA, 1978. A newly devised infra-red Ground Scanner and its application to geothermal research in volcanoes. *J. Volcanol. Geotherm. Res.*, 4, 251-264.

VOLCANOL. CENTER, SEISMOLOGICAL DIVISION, JAPAN METEOROL. AGENCY, 1979. Volcanic activity in Japan (Apr.-June, 1979) (in Japanese). *Rep. Coordinating Comm. Prediction Volcanic Eruptions*, **16**, 42.

YOKOYAMA, M., 1893a. Explosion of Azumayama (in Japanese). *J. Geography*, **5**, 533-541.

YOKOYAMA, M., 1893b. Explosion of Azumayama (in Japanese). *J. Geography*, **5**, 583-596.

29. 吾妻火山大穴火口・浄土平周辺の熱的調査

地震研究所 鍵山恒臣・萩原道徳

1979年10月に吾妻火山大穴火口・浄土平周辺において各種熱的測定を行なった．調査は赤外放射温度計による地表面温度測定，サーミスター温度計による 1 m 深地中温度測定，噴気の連続写真撮影，および目視調査からなり，これらの測定から，地熱活動の分布と熱エネルギー放出率とを把握する事を目的とした．結果は以下の通りである．

1) 燕黒沢から大穴火口に至る一帯に地熱活動域があり，それ以外の部分には熱的異常は見られなかった．

2) 同地域からの熱エネルギー放出率は，1979年10月の段階では，7.2×10^6 watt であった．この値は，地熱地帯を持つ火山，たとえば霧島火山や九重火山と比較すると，一桁小さいレベルである．

3) 吾妻火山は1977年12月の小噴火以降も活発な活動を続けていたが，1979年には，その活動も小さくなり，今回の調査時には，平常の状態であったと言われる．したがって，本報告の結果は，吾妻火山の活動が低いレベルにある時の状況を表わしていると言えよう．